Available online at www.sciencedirect.com

ScienceDirect

Ceramics International 40 (2014) 2737–2740

CERAMICS INTERNATIONAL

www.elsevier.com/locate/ceramint

Influence of LaF_3 on the crystallization and luminescence of Eu^{3+}-doped oxyfluoride glass ceramics

Chi Zhang, Shilong Zhao*, Degang Deng, Lihui Huang, Ying Tian, Shiqing Xu*

College of Materials Science and Engineering, China Jiliang University, Hangzhou 310018, China

Received 12 July 2013; received in revised form 13 October 2013; accepted 13 October 2013
Available online 22 October 2013

Abstract

The influence of LaF_3 on the crystallization behavior and luminescence of Eu^{3+} ions in the oxyfluoride borosilicate glass ceramics was investigated in details. Differential scanning calorimetry (DSC) and transmission electron microscopy (TEM) results indicated that the addition of LaF_3 decreased the glass transition temperature and promoted the crystallization of BaF_2 nanocrystals, which distributed homogeneously in the glassy matrix. A reduction of the lattice parameters of BaF_2 nanocrystals, the obvious Stark splitting of emission peaks and long fluorescence lifetime evidenced the incorporation of Eu^{3+} and La^{3+} into the BaF_2 lattice. Furthermore, experimental results indicated the distribution of Eu^{3+} ions in the oxyfluoride glass ceramics may be modified by the addition of LaF_3 content.

Keywords: Crystallization behavior; Eu^{3+} ions; Luminescence

1. Introduction

Rare earth (RE) doped optical materials have stimulated a great deal of interest due to their potential applications such as short-wavelength solid state lasers, three-dimensional display, bio-labeling and solar cells, and so on [1–3]. It is well known that the emission efficiency of RE ions is closely related to the host matrices and their crystal structures. Among various host materials, transparent oxyfluoride glass ceramics might be an ideal choice, which combine the good optical properties of RE ions in the low phonon energy fluoride crystals and suitability for industrial production of oxide glasses [4–6]. Many investigations have been carried out since the pioneering work of Wang and Ohwaki in 1993 [7]. The significant advantage is the partition of RE into the precipitated fluoride nanocrystals, which provides a local low-phonon-energy environment and strong fluorescence emissions are expected. Spectral investigation and element analysis indicate that RE is mainly enriched in the precipitated fluoride crystalline phase after the heat treatment process [8]. Eu^{3+} is known as the most sensitive probe for the rare-earth dopant site structure or symmetry due to its unique sharp emissions. In this paper, the influence of LaF_3 on the crystallization and luminescence of Eu^{3+} ions in the oxyfluoride glass ceramics was investigated in details.

2. Experimental

The precursor glasses with molar compositions are $67SiO_2$–$15B_2O_3$–$12Na_2O$–$6BaF_2$–$xLaF_3$–$0.1EuF_3$ ($x=0$, 1, 2, 3, 4), and denoted as A, B, C, D and E. Analytical pure reagents of SiO_2, H_3BO_3, Na_2CO_3, BaF_2, LaF_3 and EuF_3 were used as raw materials. Approximate 20 g batches of the mixture of raw materials were melted in a covered alumina crucible at 1400 °C for about 30 min. Then the glass was quenched into a brass mold and annealed in a furnace to release the inner stress. All the precursor glasses except the sample E were transparent and used for further investigation. In order to obtain transparent oxyfluoride glass ceramics, the precursor glasses were heat-treated at 600 °C for 2 h. The obtained glass and glass ceramics were polished for optical measurements.

*Corresponding authors. Tel.: +86 571 8683 5781; fax: +86 571 2888 9527.
E-mail addresses: shilong_zhao@hotmail.com (S. Zhao), sxucjlu@hotmail.com (S. Xu).

0272-8842/$ - see front matter © 2013 Elsevier Ltd and Techna Group S.r.l. All rights reserved.
http://dx.doi.org/10.1016/j.ceramint.2013.10.047

The DSC experiments of the precursor glasses were carried out on Netzsch DTA 404PC in N_2 atmosphere at a heating rate of 10 K/min. The precipitated crystalline phases in the oxyfluoride glass ceramics were identified by X-ray diffraction (XRD) measurements on a Bruker D2 PHASER Diffractometer with Cu-K_α radiation ($\lambda = 0.154$ nm). The microstructures of the samples were analyzed by a transmission electron microscope (TEM, JEM-2100) operating at an accelerating voltage of 200 kV. The excitation and emission spectra were measured with a Jobin–Yvon Frolog3 fluorescence spectrophotometer equipped with a 450 W Xe lamp. The decay curves of Eu^{3+} ions at 611 nm were measured by this equipment excited by a pulsed spectral LED at 370 nm, operating in the multichannel scaling mode. All measurements were collected at room temperature.

3. Results and discussion

The DSC curves of the precursor glasses with different LaF_3 contents are shown in Fig. 1a. With the increasing of LaF_3 content from 0 mol% to 3 mol%, T_g decreases gradually from 538 °C to 509 °C. A new exothermic peak appears at 590 °C for samples C and D, indicative of BaF_2 crystallization from the precursor glasses confirmed by XRD results. The exothermic peaks at around 735 °C correspond to the bulk crystallization of the glass matrix. Fig. 1b shows the XRD patterns of Eu^{3+}-doped samples heat-treated at 600 °C for 2 h. The absence of sharp crystalline peaks and two broad humps confirm the amorphous nature of the sample A. However, strong diffraction peak signals are observed in the samples with the LaF_3 addition, which indicates LaF_3 acts as nucleating agents during the nucleation process. The diffraction peaks are easily assigned to cubic BaF_2 nanocrystals (JCPDS 85-1341). From the peak width of the XRD pattern and the Scherrer formula, the mean crystalline size of BaF_2 nanocrystals were calculated to be 16.8 nm, 19.1 nm and 21.5 nm for the samples B, C and D, respectively. Obviously, the increasing LaF_3 addition promotes the growing up of BaF_2 nanocrystals, which is similar to the result in the Er^{3+}-doped SiO_2–Al_2O_3–PbF_2–ZnF_2 glass system [8]. The volume fraction of the crystalline phase (crystallinity) in the glass ceramic estimated by the ratio of integrating the area of the peaks and the total area of the XRD pattern from 10° to 80° was about 35.44%, 56.59% and 65.09% for the samples B, C and D, respectively [9,10]. In comparison with BaF_2 nanocrystals, as shown in the inset of Fig. 1b, the diffraction peaks shift gradually towards the higher angle side, exhibiting the lattice shrinkage of BaF_2 nanocrystals. It is believed that the lattice shrinkage is due to the substitution of Ba^{2+} (ionic radius 1.42 Å) by La^{3+} (ionic radius 1.16 Å) and Eu^{3+} (ionic radius 1.06 Å) in BaF_2 lattice [11].

TEM analysis was carried out to obtain the information on the morphology, size and size distribution of BaF_2 nanocrystals in the oxyfluoride glass ceramics and the results were shown in Fig. 2. The dark and spherical crystallites in the TEM images correspond to BaF_2 nanocrystals, as shown in Fig. 2a, which are homogeneously distributed in the glassy matrices. Clear lattice fringes of HRTEM image in Fig. 2b indicates the high crystallinity of BaF_2 nanocrystals. The crystalline size distribution in Fig. 2c falls in a narrow range and follows a Gaussian shaped curve with an average crystalline size of 22 nm, which agrees well with the result estimated from the XRD results.

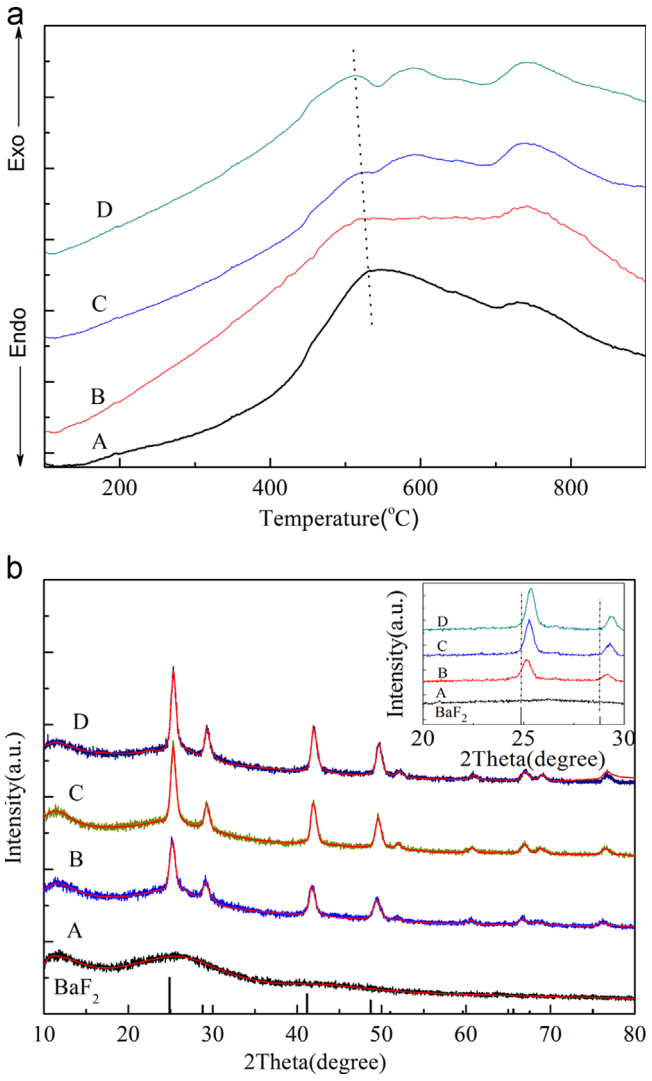

Fig. 1. (a) DSC curves and (b) XRD patterns of the samples with x mol% LaF_3 content (a) $x=0$; (b) $x=1$; (c) $x=2$; and (d) $x=3$.

In order to detect the element distribution, the energy dispersive X-ray spectroscopy(EDX) with nanosized probe of an individual BaF_2 nanocrystal and the glass matrix in 3 mol% LaF_3 doped glass ceramic were recorded and shown in Fig. 3. The appearance of Cu signal is attributed to the carbon coated copper grid used in the TEM measurement. In comparison with the EDX spectrum of the glass matrix, the spectrum of an individual BaF_2 nanocrystal exhibits relatively stronger Ba, La and F signals, and no any signal of Eu^{3+} is detected due to its too small quantity. All the results indicate that BaF_2 nanocrystals have formed in the glass matrix and La^{3+} ions are embedded in the formed BaF_2 nanocrystals after heat treatment.

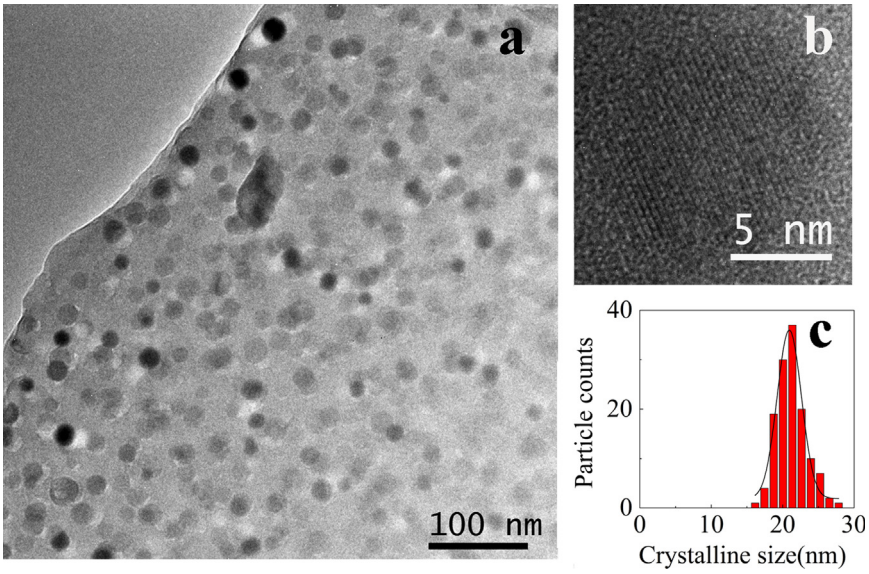

Fig. 2. (a) TEM, (b) HRTEM and (c) crystallite size distribution of BaF_2 nanocrystals in the glass ceramics.

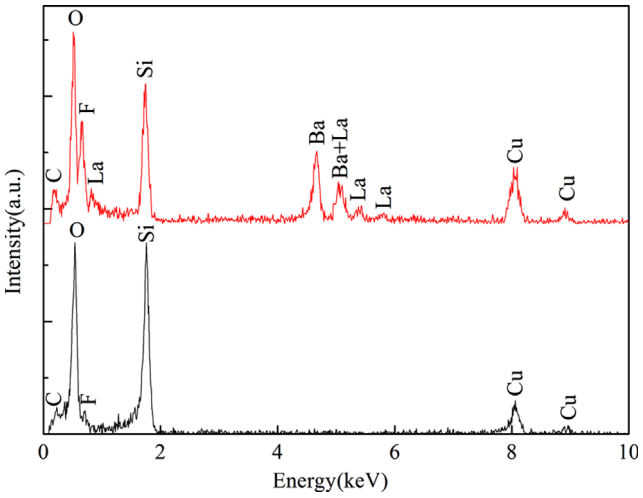

Fig. 3. EDX spectra of an individual BaF_2 nanocrystal and the glass matrix in 3 mol% LaF_3 doped glass ceramic.

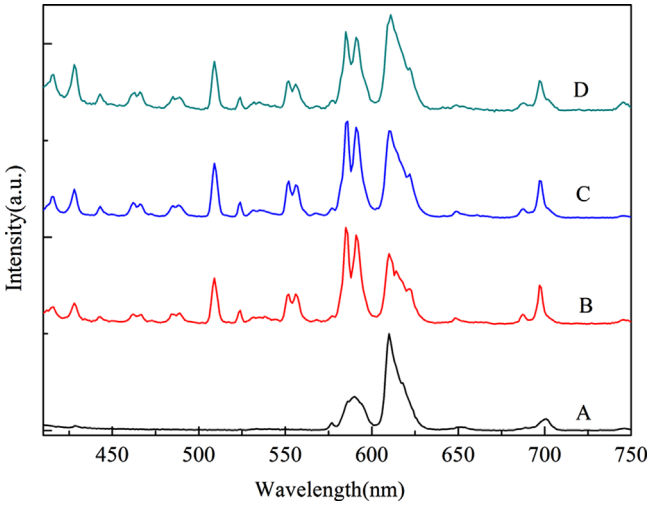

Fig. 4. Emission spectra of Eu^{3+}-doped oxyfluoride glass ceramics with (A) 0 mol%; (B) 1 mol%; (C) 2 mol%; and (D) 3 mol% addition.

The excitation spectra of Eu^{3+} monitored at 611 nm (corresponding to the transition $^5D_0 \rightarrow {}^7F_2$) indicates that the most intense excitation wavelength is located at 393 nm. Thus, the emission spectra of Eu^{3+} ions were determined under excitation at 393 nm and shown in Fig. 4. In the sample A, only the transitions $^5D_0 \rightarrow {}^7F_J$ are observed and the transitions from the higher excited states $^5D_{1,2,3}$ are quenched due to multi-phonon relaxation. However, addition of LaF_3 content results in significant changes in the emission spectra of Eu^{3+} ions. Besides the $^5D_0 \rightarrow {}^7F_J$ transitions, strong $^5D_{1,2,3} \rightarrow {}^7F_J$ transitions and strong Stark splitting at 590 nm are observed, implying that Eu^{3+} have been incorporated into the precipitated BaF_2 nanocrystals, which provide an obvious advantage of low phonon energy and decrease the multi-phonon relaxation probability. It is worth noting that there is a significant change in the relative intensities of the emission bands at 590 nm and 610 nm with the increasing of LaF_3 content. The emission peaks at 590 nm and 610 nm corresponds to the $^5D_0 \rightarrow {}^7F_1$ and $^5D_0 \rightarrow {}^7F_2$ transitions, respectively. The $^5D_0 \rightarrow {}^7F_1$ is a magnetic dipole transition and relatively insensitive to the local symmetry. The $^5D_0 \rightarrow {}^7F_2$ is a forced electric dipole transition and allowed only the condition that Eu^{3+} ions occupy a site without an inversion center, thus, it is very sensitive to the local symmetry. Therefore, the intensity ratio of the $^5D_0 \rightarrow {}^7F_2$ transition to the $^5D_0 \rightarrow {}^7F_1$ transition is regarded as a fingerprint of the variation in the incorporation of Eu^{3+} in the BaF_2 nanocrystals. The β values are calculated to be 2.855, 0.728, 0.899 and 1.306 for the samples A, B, C and D, respectively. In comparison with sample A, the decrease in β indicates the increased symmetry of the ligand field for Eu^{3+} ions, evidencing the incorporation of Eu^{3+} ions into BaF_2 lattice by substituting Ba^{2+} ions, which is consistent with the XRD results. However, the β value increase gradually with the further

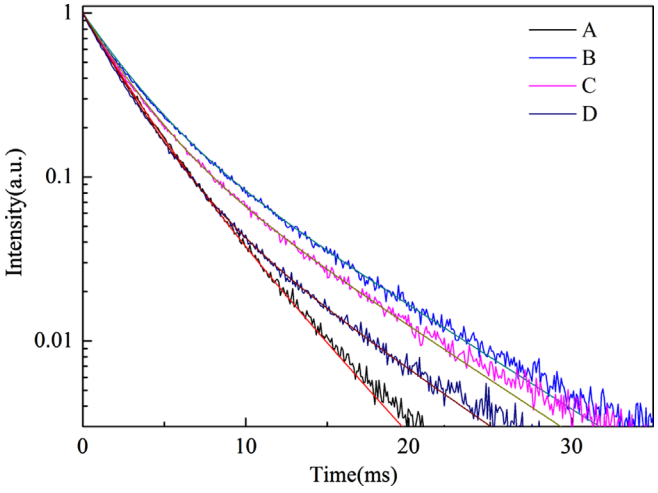

Fig. 5. Decay curves of Eu^{3+}-doped oxyfluoride glass ceramics with (A) 0 mol%; (B) 1 mol%; (C) 2 mol%; and (D) 3 mol% LaF_3 addition.

addition of LaF_3 content. Two reasons may be responsible for this change. On one hand, lattice distortion due to the addition of LaF_3 content decrease the local symmetry. On the other hand, it was found that the ionic radius of rare earth ion play an important role on the relative fraction of rare earth ions which were incorporated into the precipitated fluoride crystalline phase [12]. In an eightfold, fluoride-coordinated sites, the difference in ionic radius between Ba^{2+} and La^{3+} is smaller than that between Ba^{2+} and Eu^{3+}. Due to the smaller ion radius difference, La^{3+} ions have the priority to take the place of Ba^{2+} ions and enter into BaF_2 nanocrystals, which results in the relative content of Eu^{3+} ions partition into the BaF_2 nanocrystals and the according local symmetry decrease with the addition of LaF_3 content.

Fig. 5 shows decay curves of Eu^{3+} ions in the samples after heat-treatment at 620 °C for 2 h. For sample A, the decay curve can be approximately fitted with a single exponential function with a lifetime of 2.86 ms, which indicates that there is only one Eu^{3+} site and that Eu^{3+} ions are mainly situated in the glass matrix according to the previous XRD results. For samples B, C and D, the decay curves can only be fitted with a double-exponential function, suggesting the presence of two Eu^{3+} sites, i.e., one in the glass matrix and the other in the crystalline environment. Due to the non-exponential nature of the decay curves, the average decay lifetimes are calculated using the following equation:

$$\tau = \int_{t_0}^{\infty} \frac{I(t)}{I_{\max}} dt \quad (1)$$

where $I(t)$ is the dependence of luminescence intensity on the time t, and $I_{\max}$ is the maximum of $I(t)$ and $I(t_0)=I_{\max}$. Using the above equation, the average lifetimes have been fitted to be 3.80 ms, 3.42 ms and 3.10 ms for samples B, C and D, respectively. Evidently, the lifetime of Eu^{3+} ions exhibits the same trend to the intensity ratio of the $^5D_0 \rightarrow {}^7F_2$ transition to the $^5D_0 \rightarrow {}^7F_1$ transition.

4. Conclusions

Controlled precipitation of BaF_2 nanocrystals was achieved in the oxyfluoride borosilicate glass by the introduction of LaF_3 content, which decreased the glass transition temperature and promoted the crystallization process. The modification of the distribution of Eu^{3+} ions in the host matrix should be responsible for the change of emission spectra and fluorescence lifetime.

Acknowledgments

This work was financially supported by National Natural Science Foundation of China (51272243, 51072190 and 11004177), Zhejiang Provincial Natural Science Foundation of China (Y4110621 and Z4100030).

References

[1] D.Q. Chen, Y.S. Wang, Y.L. Yu, P. Huang, Intense ultraviolet up conversion luminescence from Tm^{3+}/Yb^{3+}: β-YF_3 nanocrystals embedded glass ceramic, Appl. Phys. Lett. 91 (2007) 051920.
[2] F. Wang, Y. Han, C.S. Lim, Y. Lu, J. Wang, J. Xu, H. Chen, C. Zhang, M. Hong, X. Liu, Simultaneous phase and size control of upconversion nanocrystals through lanthanide doping, Nature 463 (2010) 1061.
[3] M He, P Huang, C Zhang, H Hu, C Bao, G Gao, R He, D Cui, Dual phase-controlled synthesis of uniform lanthanide-doped $NaGdF_4$ upconversion nanocrystals via an OA/Ionic liquid two-phase system for in vivo dual-modality imaging, Adv. Funct. Mater. 21 (2011) 4470.
[4] A.C Yanes, A. Santana-Alonso, J. Méndez-Ramos, J Castillo, V.D. Rodríguez, Novel sol–gel nano glass ceramics comprising Ln^{3+}-doped YF_3 nanocrystals: structure and high efficient UV up-conversion, Adv. Funct. Mater. 21 (2011) 3136.
[5] S. Chen, S. Zhao, F. Zheng, C. Zhang, L. Huang, S. Xu, Enhanced up-conversion luminescence of Er^{3+}:LaOF oxyfluoride borosilicate glass ceramics, Ceram. Int. 39 (2013) 2909–2913.
[6] F.X. Xin, S.L. Zhao, S.Q. Xu, L.H. Huang, G.H. Jia, D.G. Deng, H.P. Wang, Structure and luminescence properties of Eu/Tb co-doped oxyfluoride glass ceramics containing Sr_2GdF_7 nanocrystals, Opt. Mater. 34 (2011) 85.
[7] Y. Wang, J. Ohwaki, New transparent vitro-ceramics co-doped with Er^{3+} and Yb^{3+} for efficient frequency up conversion, Appl. Phys. Lett. 63 (1993) 3268.
[8] F. Bao, Y.S. Wang, Z.J. Hu, Influence of Er^{3+} doping on microstructure of oxyfluoride glass–ceramics, Mater. Res. Bull. 40 (2005) 1645.
[9] E. Caponetti, M.L. Saladino, D. Chillura Martino, L. Pedone, S. Enzo, S. Russu, M. Bettinelli, A. Speghini, Luminescence properties of neodymium-doped yttrium aluminium garnet obtained by the co-precipitation method combined with the mechanical process, Solid State Phenom. 106 (2005) 7.
[10] L. Huang, T. Yamashita, R. Jose, Y. Arai, T. Suzuki, Y. Ohishi, Intense ultraviolet emission from Tb^{3+} and Yb^{3+} codoped glass ceramic containing CaF_2 nanocrystals, Appl. Phys. Lett. 90 (2007) 131116.
[11] D.Q. Chen, Y.L. Yu, P. Huang, H. Lin, Z.F. Shan, Y.S. Wang, Color-tunable luminescence of Eu^{3+} in LaF_3 embedded nanocomposite for light emitting diode, Acta Mater. 58 (2010) 3035.
[12] F. Goutaland, P. Jander, W.S. Brocklesby, Guojun Dai, Crystallisation effects on rare earth dopants in oxyfluoride glass ceramics, Opt. Mater. 22 (2003) 383.